Magnetization dynamics of an in-plane magnetized synthetic ferrimagnetic free layer submitted to spin-transfer torques and applied field

B. Lacoste, L. D. Buda-Prejbeanu, U. Ebels, and B. Dieny
SPINTEC, UMR CEA/CNRS/UJF-Grenoble 1/ Grenoble-INP, INAC, Grenoble F-38054, France
(Received 5 November 2013; revised manuscript received 24 January 2014; published 12 February 2014)

An equilibrium stability analysis of an in-plane magnetized synthetic ferrimagnetic free layer (SyF) submitted to multiple spin-transfer-torque (STT) influences and to applied field has been carried out. Analytical expressions for the frequency and linewidth of the excitations were derived, in the case of strong coupling between the two layers compared to the anisotropy field. The expression of the critical current for the onset of excitations in the SyF was then calculated. Above the critical current, the destabilized mode, acoustic or optical, is found to depend on the applied field direction, but also on the asymmetry of the two layers composing the SyF. A strong thickness asymmetry reduces the critical current at zero field, and allows to select the destabilized mode. The critical current of an in-plane SyF with mutual spin torque between the layers and without reference layer was computed. For a symmetric SyF, the optical mode is the only mode that can be destabilized by STT.

DOI: 10.1103/PhysRevB.89.064408 PACS number(s): 75.70.Cn, 75.78.−n, 85.70.Kh

I. INTRODUCTION

Spin-transfer torque [1,2] (STT) in magnetic tunnel junctions (MTJ) is particularly interesting for manipulating the magnetization in spintronic devices. Indeed, via the STT phenomenon, the magnetization can pump energy into the spin current and be driven into a very original dynamics behavior. There are two main applications for STT devices: magnetic random access memory (STT-MRAM) [3,4] and STT nano-oscillators (STO) [5–8]. In both cases, the free layer magnetization, in equilibrium when no current is flowing through the device, gets destabilized by the spin transfer torque from the reference layer when a current starts flowing through the structure with appropriate polarity. The free layer magnetization then switches or remains in a dynamical state of self-sustained oscillations. In the case of an in-plane magnetized free layer with in-plane reference layer, the dynamics is well-described by the Landau-Lifshitz-Gilbert equation with additional STT terms. Stability analysis of the equilibrium configuration successfully predicts the critical currents and FMR oscillations frequency in such structures. However, analytical expressions of the critical currents are only known if the free layer is composed of a single ferromagnetic layer [9,10].

In this paper, we analyze the magnetization dynamics of a synthetic ferrimagnetic (SyF) composite free layer, composed of two in-plane magnetized layers coupled by Ruderman-Kittel-Kasuya-Yosida (RKKY) interaction. SyF layers with antiparallel coupling are interesting because of their reduced magnetostatic stray fields. Thus using SyF layers in nanopillars allows to reduce the magnetostatic influence of adjacent layers.

If the effect of an external field on the stability of a SyF free layer is well-documented [9], the STT-induced excitations are not fully understood. Here, we present a general equilibrium stability analysis of the SyF free layer, which consists in finding the eigenvalues of the 4×4 dynamical matrix. In the case of a large RKKY coupling compared to the anisotropy fields, which is generally the case in MRAM and STO stacks, analytical expressions of the eigenvalues can be computed with a good approximation. This is achieved by solving approximately the quartic equation of the characteristic polynomial, in the limit of a small damping parameter α. This allowed us to obtain the expression of the critical current for a SyF free layer and, also, to determine which mode, acoustic or optical, is excited by the current in the FMR limit. In previous papers, the critical currents of a SyF could be obtained either only at zero applied field and for symmetric layers [9], or only for the specific applied field at which the two modes, acoustic and optical, have the same critical current [10]. Contrary to these previous studies, the analytical expression of the critical current in the most general case and for any applied field could be computed. These analytical expressions give insights on the contribution of each physical or material parameter.

To illustrate the importance of knowing the analytical expressions of the critical current of a SyF, we focused on two representative systems: (i) an MTJ composed of an in-plane SyF free layer and of a fixed in-plane reference layer for memory application. We show that the critical currents of strongly asymmetric SyF are lower than in single layers with the same magnetic volume. (ii) The second is a SyF with mutual spin torque between the two layers and without reference layer, for oscillator application.

II. EQUILIBRIUM STABILITY ANALYSIS

A. Description of the model and parameters

The free layer is composed of two coupled magnetic layers, labeled 1 and 2, as described in Fig. 1. The total free energy E holds the demagnetizing energy of both layer, the uniaxial anisotropy and the Zeeman energy due to the in-plane field applied along the easy axis, plus an RKKY interaction term. The magnetization of layer 1 (2) is labeled $\boldsymbol{m}_1$ ($\boldsymbol{m}_2$), its saturation magnetization M_1 (M_2), its volume $V_1 = t_1 S$ (V_2) with thickness t_1 (t_2) and area S, its demagnetizing field H_{d1} (H_{d2}), and its anisotropy field H_{k1} (H_{k2}), assumed to be along the x axis. The external field $H_{x1} = H_a + H_{ex1}$ ($H_{x2} = H_a + H_{ex2}$) is composed of the sum of the in-plane applied field H_a that is common to the two layers, and a bias field H_{ex1} (H_{ex2}) assumed for generality to be different in the two layers. These bias fields can have various origins (magnetostatic coupling to the reference layer, exchange bias

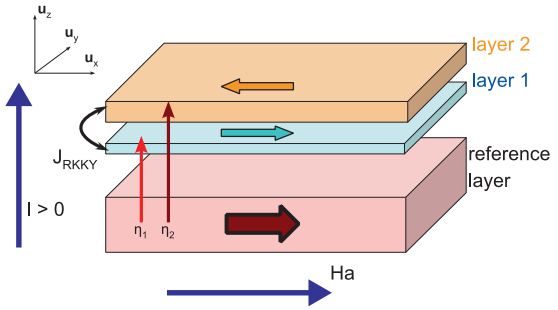

FIG. 1. (Color online) Schematics of the synthetic ferrimagnet (SyF) as a free layer with a fixed in-plane magnetized reference layer.

to an additional antiferromagnetic layer, etc.):

$$E = \tfrac{1}{2}\mu_0 V_1 M_1 H_{d1}(\boldsymbol{m}_1\cdot\boldsymbol{u}_z)^2 - \tfrac{1}{2}\mu_0 V_1 M_1 H_{k1}(\boldsymbol{m}_1\cdot\boldsymbol{u}_x)^2 - \mu_0 V_1 M_1 H_{x1}\boldsymbol{m}_1\cdot\boldsymbol{u}_x + \tfrac{1}{2}\mu_0 V_2 M_2 H_{d2}(\boldsymbol{m}_2\cdot\boldsymbol{u}_z)^2 - \tfrac{1}{2}\mu_0 V_2 M_2 H_{k2}(\boldsymbol{m}_2\cdot\boldsymbol{u}_x)^2 - \mu_0 V_2 M_2 H_{x2}\boldsymbol{m}_2\cdot\boldsymbol{u}_x - S J_{\mathrm{RKKY}}\boldsymbol{m}_1\cdot\boldsymbol{m}_2, \quad (1)$$

where J_{RKKY} is the Ruderman-Kittel-Kasuya-Yosida (RKKY) coupling energy per unit area. A negative J_{RKKY} corresponds to an antiferromagnetic coupling between the layers. With an antiferromagnetic coupling, $J_{\mathrm{ex}} < 0$, the two stable equilibrium configurations are defined by ($\boldsymbol{m}_1 = \boldsymbol{u}_x$, $\boldsymbol{m}_2 = -\boldsymbol{u}_x$), called parallel P, and ($\boldsymbol{m}_1 = -\boldsymbol{u}_x$, $\boldsymbol{m}_2 = \boldsymbol{u}_x$), called antiparallel AP, P, and AP referring to the orientation of the magnetization in layer 1 relatively to that of the reference layer. With a ferromagnetic coupling, $J_{\mathrm{ex}} > 0$, the equilibriums are ($\boldsymbol{m}_1 = \boldsymbol{u}_x$, $\boldsymbol{m}_2 = \boldsymbol{u}_x$) for P, and ($\boldsymbol{m}_1 = -\boldsymbol{u}_x$, $\boldsymbol{m}_2 = -\boldsymbol{u}_x$) for AP.

We introduce what we call the spin-torque potentials of each layer, which account for the spin-transfer torque effect on the magnetization dynamics of the layers [11]. These spin-torque potentials simplify the expressions, as they are independent of the choice of basis, and give exactly the same expressions as the usual formalism (see Appendix A). The spin-torque potentials P_1 and P_2 are defined for each layer. They include the spin torque due to the reference layer on the two layers, and the mutual spin torque:

$$P_1 = -\frac{\hbar}{2e} I \frac{\eta_1}{\lambda_1}\ln(1+\lambda_1\boldsymbol{m}_1\cdot\boldsymbol{u}_x) + \frac{\hbar}{2e} I \eta_{21}\boldsymbol{m}_1\cdot\boldsymbol{m}_2, \quad (2)$$

$$P_2 = -\frac{\hbar}{2e} I \frac{\eta_2}{\lambda_2}\ln(1+\lambda_2\boldsymbol{m}_2\cdot\boldsymbol{u}_x) - \frac{\hbar}{2e} I \eta_{12}\boldsymbol{m}_1\cdot\boldsymbol{m}_2. \quad (3)$$

Here, a positive current corresponds to electrons flowing from layer 2 towards layer 1, and then to the reference layer. The spin polarization and spin polarization asymmetry due to the reference layer on layer 1 (layer 2) are labeled η_1 (η_2) and λ_1 (λ_2, respectively). η_2 in general is expected to be much smaller than η_1 since the spin-polarized electrons originating from the reference layer get spin-reoriented within a distance of the order of 1 nm when traversing layer 1. However, if layer 1 is sufficiently thin, a STT influence from the reference layer on layer 2 may still exist [12,13]. However, η_2 will be neglected in the second part of the paper. The spin polarization of the current due to layer 1 (layer 2) that induces a torque on layer 2 (layer 1) is labeled η_{12} (η_{21}, respectively). The spin polarization asymmetry is assumed to vanish for the mutual spin torque. Notice the minus sign in front of the mutual spin-torque term (last term) in P_2, and the plus sign in P_1, because the layer 2 receives reflected electrons from layer 1, whereas layer 1 receives direct electrons from layer 2 for positive current.

The Landau-Lifshitz-Gilbert-Slonczewski (LLGS) equation reads

$$\mu_0 V_1 M_1 \frac{\mathrm{d}\boldsymbol{m}_1}{\mathrm{d}t} = \gamma_1\boldsymbol{m}_1\times\boldsymbol{\partial}_{\boldsymbol{m}_1}(E+\beta\alpha_1 P_1) + \gamma_1\boldsymbol{m}_1\times\{\boldsymbol{m}_1\times[\boldsymbol{\partial}_{\boldsymbol{m}_1}(\alpha_1 E - P_1)]\},$$

$$\mu_0 V_2 M_2 \frac{\mathrm{d}\boldsymbol{m}_2}{\mathrm{d}t} = \gamma_2\boldsymbol{m}_2\times\boldsymbol{\partial}_{\boldsymbol{m}_2}(E+\beta\alpha_2 P_2) + \gamma_2\boldsymbol{m}_2\times\{\boldsymbol{m}_2\times[\boldsymbol{\partial}_{\boldsymbol{m}_2}(\alpha_2 E - P_2)]\},$$

where α_1 and α_2 are the damping constants of the layers. For $i = (1,2)$, $\gamma_i = \frac{\mu_0\gamma}{1+\alpha_i^2}$, with γ the gyromagnetic ratio. We consider that $\gamma_1 = \gamma_2 = \mu_0\gamma$. The adimensional term β accounts for possible interlayer exchange coupling (IEC), or fieldlike spin torque. See Appendix A for the definition of β.

Without applied current, the free layer magnetization is in one of the two equilibrium configurations, P or AP. When a current is applied, the equilibrium may become unstable. The stability of the equilibrium is studied by linearizing the LLGS equation around the equilibrium position. The eigenvalues of the 4×4 dynamical matrix L, obtained by differentiating the LLGS vector field (see Appendix B), correspond to the FMR eigenmodes. The FMR eigenfrequency and linewidth correspond to the imaginary part and the double of the real part of the eigenvalues of L, respectively.

In the following, we use simplified notation to represent the average quantities over the two layers and the asymmetric quantities:

$$n = \mathrm{sign}(J_{\mathrm{RKKY}}), \quad m = \cos\phi_1,$$

$$\omega = \gamma_0(H_{d2}+H_{d1})/2, \quad \epsilon = \frac{H_{d2}-H_{d1}}{H_{d2}+H_{d1}},$$

$$\alpha = (\alpha_2+\alpha_1)/2, \quad \zeta = \frac{\alpha_2-\alpha_1}{\alpha_2+\alpha_1},$$

$$b_1 = \frac{\gamma_0}{\omega}\left[H_{k1} + m(H_a+H_{ex1}) + \frac{|J_{\mathrm{RKKY}}|}{\mu_0 M_1 t_1}\right],$$

$$b_2 = \frac{\gamma_0}{\omega}\left[H_{k2} + nm(H_a+H_{ex2}) + \frac{|J_{\mathrm{RKKY}}|}{\mu_0 M_2 t_2}\right],$$

$$Q = \frac{b_2+b_1}{2}, \quad \kappa = \frac{b_2-b_1}{b_2+b_1},$$

$$j_1 = \frac{\gamma|J_{\mathrm{RKKY}}|}{\omega M_1 t_1}, \quad j_2 = \frac{\gamma|J_{\mathrm{RKKY}}|}{\omega M_2 t_2},$$

$$j = (j_2+j_1)/2, \quad \nu = \frac{j_2-j_1}{j_2+j_1}, \quad J = \sqrt{j_1 j_2},$$

$$i_1 = \frac{mI}{1+m\lambda_1}\frac{\gamma\hbar}{2e\omega S}\frac{\eta_1}{\alpha_1 M_1 t_1},$$

$$i_2 = \frac{nmI}{1+nm\lambda_2}\frac{\gamma\hbar}{2e\omega S}\frac{\eta_2}{\alpha_2 M_2 t_2},$$

$$i = (i_2 + i_1)/2, \quad \mu = \frac{i_2 - i_1}{i_2 + i_1},$$

$$k_{21} = \frac{nI}{1 + n\lambda_{21}} \frac{\gamma\hbar}{2e\omega S} \frac{\eta_{21}}{\alpha_1 M_1 t_1},$$

$$k_{12} = \frac{nI}{1 + n\lambda_{12}} \frac{\gamma\hbar}{2e\omega S} \frac{\eta_{12}}{\alpha_2 M_2 t_2},$$

$$k = \frac{k_{12} + k_{21}}{2}, \quad \rho = \frac{k_{12} - k_{21}}{k_{12} + k_{21}}.$$

$$L = \omega \begin{pmatrix} -\alpha_1(1 - \epsilon + b_1 + i_1 - k_{21}) & -b_1 + \beta\alpha_1^2(i_1 - k_{21}) & \alpha_1 n(j_1 - k_{21}) & j_1 + \beta\alpha_1^2 k_{21} \\ 1 - \epsilon + b_1 - \beta\alpha_1^2(i_1 - k_{21}) & -\alpha_1(b_1 + i_1 - k_{21}) & -n\left(j_1 + \beta\alpha_1^2 k_{21}\right) & \alpha_1(j_1 - k_{21}) \\ \alpha_2 n(j_2 + k_{12}) & j_2 - \beta\alpha_2^2 k_{12} & -\alpha_2(1 + \epsilon + b_2 + i_2 + k_{12}) & -b_2 + \beta\alpha_2^2(i_2 + k_{12}) \\ -n\left(j_2 - \beta\alpha_2^2 k_{12}\right) & \alpha_2(j_2 + k_{12}) & 1 + \epsilon + b_2 - \beta\alpha_2^2(i_2 + k_{12}) & -\alpha_2(b_2 + i_2 + k_{12}) \end{pmatrix}.$$

It is important to notice that the dynamical matrix L can be separated in four 2×2 blocks. The top left (respectively, bottom-right) correspond to the dynamical matrix of the layer 1 (respectively, layer 2) alone, the other layer being fixed. Due to the RKKY interaction, the block corresponds to an isolated layer with exchange field coming from the coupling with the fixed layer. The two other 2×2 blocks contain only interaction terms proportional to the RKKY coupling.

To calculate the eigenvalues, one needs to solve a quartic equation. The fact that the eigenvalues are expected to be two pairs of complex-conjugate values implies that the quartic equation can be factorized into two quadratic equations. Hence the four eigenvalues are given by the following general expressions:

$$\lambda_i = \frac{\mathfrak{t}_1}{4} \pm_1 \frac{\sqrt{W}}{2} \pm_2 \frac{i}{2} \sqrt{2\mathfrak{a} + W \pm_1 \frac{2\mathfrak{b}}{\sqrt{W}}}. \tag{4}$$

The four possibilities of the couples $\pm_1$ and $\pm_2$ yield four independent solutions, where $\pm_2$ distinguishes two complex-conjugate values. Here, the quantity W is real positive, hence the real part of the eigenvalues (corresponding to half of the linewidth) is given by the sum of the first and second terms. The imaginary part is given by the square-root term. This assumption is valid if the expression inside the radical is positive, which is supposed to be always the case here, otherwise it means that the FMR frequency vanishes. Whereas the parameter $\pm_2$ differentiates two complex conjugates eigenvalues, the parameter $\pm_1$ differentiates two eigenmodes of the SyF, the so-called optical and acoustic modes, which are associated to different eigenvectors. The optical mode is defined to be the mode with the highest frequency. By looking numerically at the eigenvectors of the optical mode, it appears that the in-plane angles of the two layers magnetization with respect to the x axis are in phase, whereas the out-of-plane angles are in antiphase, and vice versa for the acoustic mode.

The parameters of Eq. (4) depend on the coefficients of the characteristic polynomial of degree four. These coefficients are polynomial functions of the matrix traces of powers of the dynamical matrix L. Considering $\alpha \ll 1$ (except for $\mathfrak{b}$, that we calculate up to the third order in α), they are given by

$$\mathfrak{t}_1 = \mathrm{trace}(L), \quad \mathfrak{t}_2 = \mathrm{trace}(L^2), \quad \mathfrak{t}_3 = \mathrm{trace}(L^3),$$

$$\mathfrak{a} = -\tfrac{1}{2}\mathfrak{t}_2 + \tfrac{1}{8}\mathfrak{t}_1^2 \approx -\tfrac{1}{2}\mathfrak{t}_2,$$

$$\mathfrak{b} = -\tfrac{1}{3}\mathfrak{t}_3 + \tfrac{1}{4}\mathfrak{t}_1\mathfrak{t}_2 - \tfrac{1}{24}\mathfrak{t}_1^3,$$

$$\mathfrak{d} = \tfrac{5}{48}\mathfrak{t}_1^4 - \tfrac{1}{2}\mathfrak{t}_1^2\mathfrak{t}_2 + \tfrac{1}{4}\mathfrak{t}_2^2 + \tfrac{1}{3}\mathfrak{t}_1\mathfrak{t}_3 - 4\det(L),$$

$$\approx \tfrac{1}{4}\mathfrak{t}_2^2 - 4\det(L),$$

and W is the solution of the cubic equation

$$W^3 + 2\mathfrak{a}W^2 + \mathfrak{d}W - \mathfrak{b}^2 = 0. \tag{5}$$

In most cases, the polynomial of Eq. (5) can be reduced to a linear equation, because the parameter $\mathfrak{b}$ is small (it is of order α in ω unit) compared to $\mathfrak{a}$ and $\mathfrak{d}$ (of order 1 in ω unit).

For small RKKY coupling energy per unit area compared to the anisotropy energy per unit area ($H_k M_s t$), namely $J_{\mathrm{RKKY}} \approx 1 \times 10^{-5}$ J/m^2 for $H_k = 20$ kA/m, $M_s = 1.2 \times 10^6$ A/m, and $t \approx 3$ nm, the cubic equation may be approximated by a quadratic equation by dropping the W^3 term to get a good approximation of the solution.

For relatively high RKKY coupling, $J_{\mathrm{RKKY}} \approx 1 \times 10^{-4}$ J/m^2 or larger, the W^2 term can also be dropped and the solution W of Eq. (5) has the following expression:

$$W = \frac{\mathfrak{b}^2}{\mathfrak{d}}.$$

The two modes, optical and acoustic, have different frequencies, but also different linewidths, which are twice the real part of λ_i. Let ω_{op}, ω_{ac}, $\Delta\omega_{\mathrm{op}}$, and $\Delta\omega_{\mathrm{ac}}$ be the eigenfrequency and linewidth of the optical and acoustic modes. They are given by

$$\omega_{\mathrm{op}} = \sqrt{\frac{\mathfrak{a}}{2} + \frac{\sqrt{\mathfrak{d}}}{2}}, \quad \omega_{\mathrm{ac}} = \sqrt{\frac{\mathfrak{a}}{2} - \frac{\sqrt{\mathfrak{d}}}{2}}, \tag{6}$$

$$\Delta\omega_{\mathrm{op}} = \frac{\mathfrak{t}_1}{2} + \frac{\mathfrak{b}}{\sqrt{\mathfrak{d}}}, \tag{7}$$

$$\Delta\omega_{\mathrm{ac}} = \frac{\mathfrak{t}_1}{2} - \frac{\mathfrak{b}}{\sqrt{\mathfrak{d}}}. \tag{8}$$

B. Calculating the eigenvalues of the dynamical matrix

The dynamical matrix is evaluated at the two equilibrium positions, ($\theta_1 = \theta_2 = \pi/2$, $\cos\phi_1 = \pm 1$, $\cos\phi_2 = \pm 1$), labeled by the parameter $m = \cos\phi_1$: $m = 1$ is the parallel (P) equilibrium state, $m = -1$ is the antiparallel (AP) equilibrium state. If $n = 1$, the two layers of the SyF are parallel at equilibrium, if $n = -1$, there are antiparallel. In the later configuration, the system is called a synthetic antiferromagnet (SAF), it is widely used for memory and nano-oscillator applications:

Neglecting the terms of order superior to 1 in α, the quantities $\mathfrak{t}_1$, $\mathfrak{a}$, $\mathfrak{d}$, and $\mathfrak{b}$ are given by

$$\mathfrak{t}_1 = -2\alpha\omega[1+2Q+2i+2\rho k+\zeta(\epsilon+2\mu i+2\kappa Q+2k)],$$

$$\mathfrak{a} = 2\omega^2[Q(1+Q)+(\kappa Q)^2+\epsilon\kappa Q+nJ^2],$$

$$\mathfrak{d} = 4\omega^4 J^2\left\{\left(\frac{Q}{J}\right)^2[\epsilon+\kappa(1+2Q)]^2+\frac{1+n}{2}[(1+2Q)^2-\epsilon^2]+\frac{1-n}{2}[1-(\epsilon+2\kappa Q)^2]\right\},$$

$$\mathfrak{b} = -2\alpha\omega^3\Bigg(Q[\epsilon+\kappa(1+2Q)][\epsilon+2\mu i+2\kappa Q+2k+\zeta(1+2i+2Q+2\rho k)]+2\left(\frac{1+n}{2}\right)(1+2Q)[J^2+kj(\rho-\nu)$$
$$+\zeta kj(1-\rho\nu)]-\frac{1-n}{2}(\epsilon+2\kappa Q)\{2kj(1-\rho\nu)+2\zeta[J^2+kj(\rho-\nu)]\}\Bigg).$$

For symmetric systems without fixed reference layer and with mutual spin torque, $\mathfrak{b}$ vanishes. Hence we need the term of order 3 in α of $\mathfrak{b}$. Assuming the two layers have the same damping parameter ($\zeta = 0$), the third order of parameter $\mathfrak{b}$ is given by

$$\mathfrak{b}_{\alpha^3} = 2\alpha^3\omega^3\Bigg\{(\epsilon+2\kappa Q+2k+2\mu i)\times\left(\frac{\epsilon}{2}+\beta[(k+\mu i)(1+2Q)+(i+\rho k)(\epsilon+2\kappa Q)]\right)$$
$$+\left(\frac{1+n}{2}\right)2\beta[(1+2Q+2i+2\rho k)kj(\rho-\nu)-(1+2Q)k^2(1-\rho^2)+j^2(1-\nu^2)(2i+2\rho k)]$$
$$+\left(\frac{1-n}{2}\right)2\beta kj(1-\rho\nu)(\epsilon+2\kappa Q-2k-2\mu i)\Bigg\}.$$

To illustrate the validity of these expressions in the approximation of relatively strong RKKY coupling, Fig. 2 shows the error between the analytical expression of the linewidth and the values extracted from the numerical eigenvalues computation of the 4×4 matrix L. The linewidth versus applied current is computed for a symmetric SyF, with an anisotropy field of $H_k = 20$ kA/m and a small applied field $H_a = 2$ kA/m to differentiate the two modes. Figure 2(a), with $J_{\mathrm{RKKY}} = -1\times10^{-4}$ J/m^2, shows a good agreement between the analytical and numerical expression, whereas in Fig. 2(b), with $J_{\mathrm{RKKY}} = -1\times10^{-5}$ J/m^2, the two expressions differ, especially for large currents.

The expressions of the eigenfrequencies for the two modes, optical and acoustic, are independent of α at the first order. Therefore they could be extracted from the dynamical matrix of the conservative part alone. With only the conservative part, the 4×4 dynamical matrix has several vanishing coefficients, so it is easier to compute its determinant. The eigenfrequencies are consistent with previous publications [9] that do not take the dissipative part into account. At the first order in α, they are given by

$$\frac{\omega^2_{\mathrm{op/ac}}}{\omega^2} = Q(1+Q)+\kappa^2Q^2+\epsilon\kappa Q+nJ^2$$
$$\pm\sqrt{Q^2[\epsilon+\kappa(1+2Q)]^2+\frac{1+n}{2}J^2[(1+2Q)^2-\epsilon^2]+\frac{1-n}{2}J^2[1-(\epsilon+2\kappa Q)^2]}. \quad (9)$$

III. STABILITY ANALYSIS OF A SYF WITH REFERENCE LAYER

A. Critical currents of the two modes

According to these expressions, ω_{op} and ω_{ac} are independent of the applied current up to order 1 in α, the current dependence of the eigenfrequencies is of order $\alpha^2 I$. Moreover, the difference of the squared frequencies of the two modes is proportional to the RKKY coupling:

$$\delta\omega^2 = \omega^2_{\mathrm{op}}-\omega^2_{\mathrm{ac}} = 2\omega^2 J\sqrt{\gamma_n}$$
$$\text{with}\gamma_n = \mathfrak{d}/(4\omega^4J^2)\approx 1.$$

The critical current for the optical and acoustic modes are computed by solving $\Delta\omega_{\mathrm{op}} = 0$ and $\Delta\omega_{\mathrm{ac}} = 0$. However, the linewidths of the two modes are different, so the critical current characterizing the onset of the excitations is given by the smallest of the two currents.

In the case of two layers with the same damping constant, $\zeta = 0$, and without mutual spin torque, the critical current (either optical or acoustic) is given by

$$\left|i^c_{\mathrm{op/ac}}\right| = \frac{1/2+Q\pm(\kappa Q+\epsilon/2)\delta}{1\pm\mu\delta},$$

where $\delta = \frac{Q}{J\sqrt{\gamma_n}}[\epsilon+\kappa(1+2Q)]$.

Notice that the critical currents of the two modes are equal for $\delta = 0$. The critical current is also maximum if $\delta = 0$. This maximal critical current was computed by Baláž *et al.* [10] using another method, which provides an analytical expression only for the maximal critical current though. Their expression is in agreement with the expressions presented in this paper.

In order to decrease the critical current in a SyF, we need to increase the denominator of the previous expression, by increasing δ. Hence there are two different options to reduce the critical current in a SyF: (i) increasing the demagnetizing field mismatch ϵ; (ii) increasing the mismatch κ, by increasing

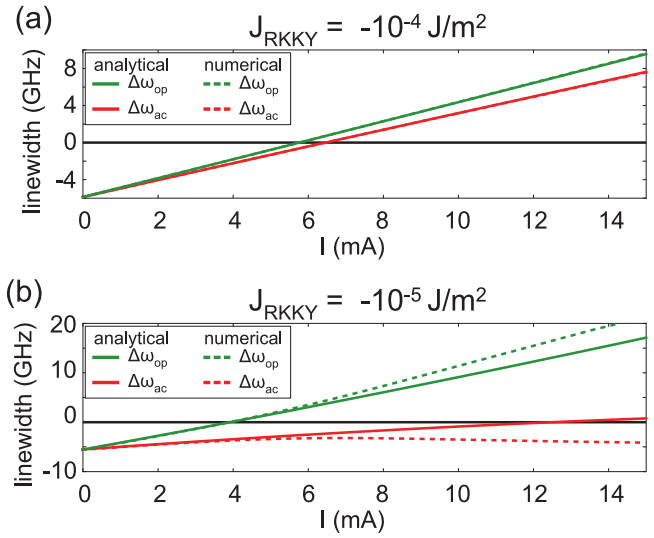

FIG. 2. (Color online) Comparison of the analytical (full lines) and numerical (dotted lines) real parts of the eigenvalues of the two modes, optical (upper green lines) and acoustic (lower red lines) of a symmetric SyF with different RKKY coupling: (a) $J_{\mathrm{RKKY}} = -1 \times 10^{-4}$ and (b) -1×10^{-5} J/m^2. The other parameters are $H_a = 2$ kA/m, $\alpha = 0.02$, $M_S = 1.2e6$ A/m, $H_{d1} = H_{d2} = 1.2e6$ A/m, $H_{k1} = H_{k2} = 20e3$ A/m, $\eta_1 = 0.3$, and $S = 10^{-14}$ m^2.

the uniaxial anisotropy mismatch, or inducing an exchange bias field on one of the ferromagnetic layer by coupling it to an antiferromagnetic layer, or increasing the layers thickness mismatch. The three cases (the uniaxial anisotropy mismatch is not treated) are represented in Fig. 3.

In this figure, the phase diagram of the single layer and SyF free layers versus applied current and field, obtained from macrospin simulations, is compared to the analytical expressions. The diagrams represent the average in-plane component along the easy axis of the first layer magnetization $\langle m_x^1 \rangle$, the one that is the closest to the reference layer. This component is related to the TMR, so it represents a physical measurable parameter. The average of m_x^1 is taken between 8 and 10 ns of the 10-ns long current pulse. Hence the results are supposed to reflect less of the transient regime, and more of the steady state reached after the pulse is applied. The magnetization is initially in the P configuration: $m_x^1 = 1$, represented in red on the graphs. The AP configuration ($m_x^1 = -1$) is represented in blue. The simulation parameters are summarized in Appendix C.

Figure 3(a) represents the phase diagram of a single layer (SL) free layer, initially in the P configuration. The simulation parameters are $\alpha = 0.02$, $M_S = 1.2 \times 10^6$ A/m, $H_k = 20 \times 10^3$ A/m, $H_{ex} = 0$, $\eta_1 = 0.3$, $\lambda_1 = 0$, $S = 10^{-14}$ m^2, and $t = 3$ nm. The magnetization is reversed for a density of current around 5×10^{11} A/m^2 (5 mA with an area $S = 100 \times 100$ nm^2) at zero field. Only one direction of the field, negative fields, switches the free layer. The other field direction stabilizes the free layer in the P configuration. The calculated critical line is in good agreement with the simulations. Notice that the calculated critical line is composed of two parts: (i) a "horizontal" line that corresponds to the vanishing of the FMR eigenfrequency (its equation is given by $H_a = H_k$) and (ii) the critical current linear with respect to the field, that comes from the vanishing of the linewidth $\Delta\omega$. Its expression is given by $I_c = \frac{\alpha}{\eta_1}\frac{2e}{\hbar}\mu_0 M_S V(\frac{H_d}{2} + H_k + H_a)$ [9]. For large positive fields ($H_a > 10$ kA/m), the magnetization is destabilized into an in-plane precession (IPP) state instead of switching just above the critical current.

Figure 3(b) is the phase diagram of a symmetric SyF, initially in the P state ($m_x^1 = 1$, $m_x^2 = -1$). The simulation parameters are $\alpha = 0.02$ ($\alpha_1 = \alpha_2$), $M_S = 1.2 \times 10^6$ A/m ($M_{S1} = M_{S2}$), $H_{d1} = H_{d2} = 1.2 \times 10^6$ A/m, $H_{k1} = H_{k2} = 20 \times 10^3$ A/m, $H_{ex1} = H_{ex2} = 0$ A/m, $\eta_1 = 0.3$, $\eta_2 = 0$, $t_1 = t_2 = 1.5$ nm, $J_{\mathrm{RKKY}} = -1 \times 10^{-3}$ J/m^2. These parameters are the same for Figs. 3(c)–3(f), except otherwise mentioned. The calculated critical line for the acoustic mode (red dotted line) and the optical mode (green dashed line) are in agreement with the simulations. The optical critical line is defined by the vanishing of the optical linewidth, $\Delta\omega_{\mathrm{op}} = 0$. The acoustic critical line is composed of two parts, like in the single layer case: (i) two horizontal lines, corresponding to the vanishing of the acoustic eigenfrequency ω_{ac}. The two critical field values, for positive and negative field can be different, as seen in the other graphs of Fig. 3. In the symmetric case, they have the same absolute value. The critical fields are defined by the vanishing of Eq. (9). (ii) The second part corresponds to the vanishing of the acoustic linewidth, $\Delta\omega_{\mathrm{ac}} = 0$. It is defined by Eq. (10).

Notice that the calculated critical lines are also in agreement with the critical lines computed by extracting numerically the eigenvalues of the dynamical matrix, which are not shown on these graphs because they superpose with the calculated lines. This is because the condition of a large RKKY coupling is fulfilled, as it was stated previously (see Fig. 2).

For negative fields, the acoustic critical current is smaller than the optical critical current. Just above the acoustic critical current, the magnetization is destabilized following the acoustic mode, and it reaches an IPP steady state, with an oscillation frequency close to the acoustic FMR frequency. For currents slightly larger than the acoustic critical current, the IPP state does not survive and the magnetization switches. The range of IPP state is not clearly visible on the graph because of its small current range. It spans close to the border between P and AP region in negative fields. For positive fields, the optical critical current is smaller than the acoustic critical current. Hence, above the optical critical current, the magnetization is destabilized and grows away from the equilibrium with optical-like oscillations, to eventually switch.

For a symmetric SyF as described in Fig. 3(b), the evolutions of the transverse in-plane components of the magnetization, m_{1y} and m_{2y}, above the optical and acoustic critical lines are shown in Fig. 4. The destabilization mode is different in the two cases, positive and negative fields of $H_a = \pm 50$ kA/m, and with the same applied current of $I = 9.2$ mA (above the critical current in both cases). For positive fields, the mode is optical, characterized by a high oscillation frequency and in-phase transverse in-plane components. On the contrary, for negative fields, the mode is acoustic, with a lower frequency and out-of-phase in-plane transverse components.

Figures 3(c)–3(f) show the phase diagram of asymmetric SyF. In Fig. 3(c), the layer 2 is subjected to an exchange bias field of $H_{ex2} = -50$ kA/m, all the other simulation parameters

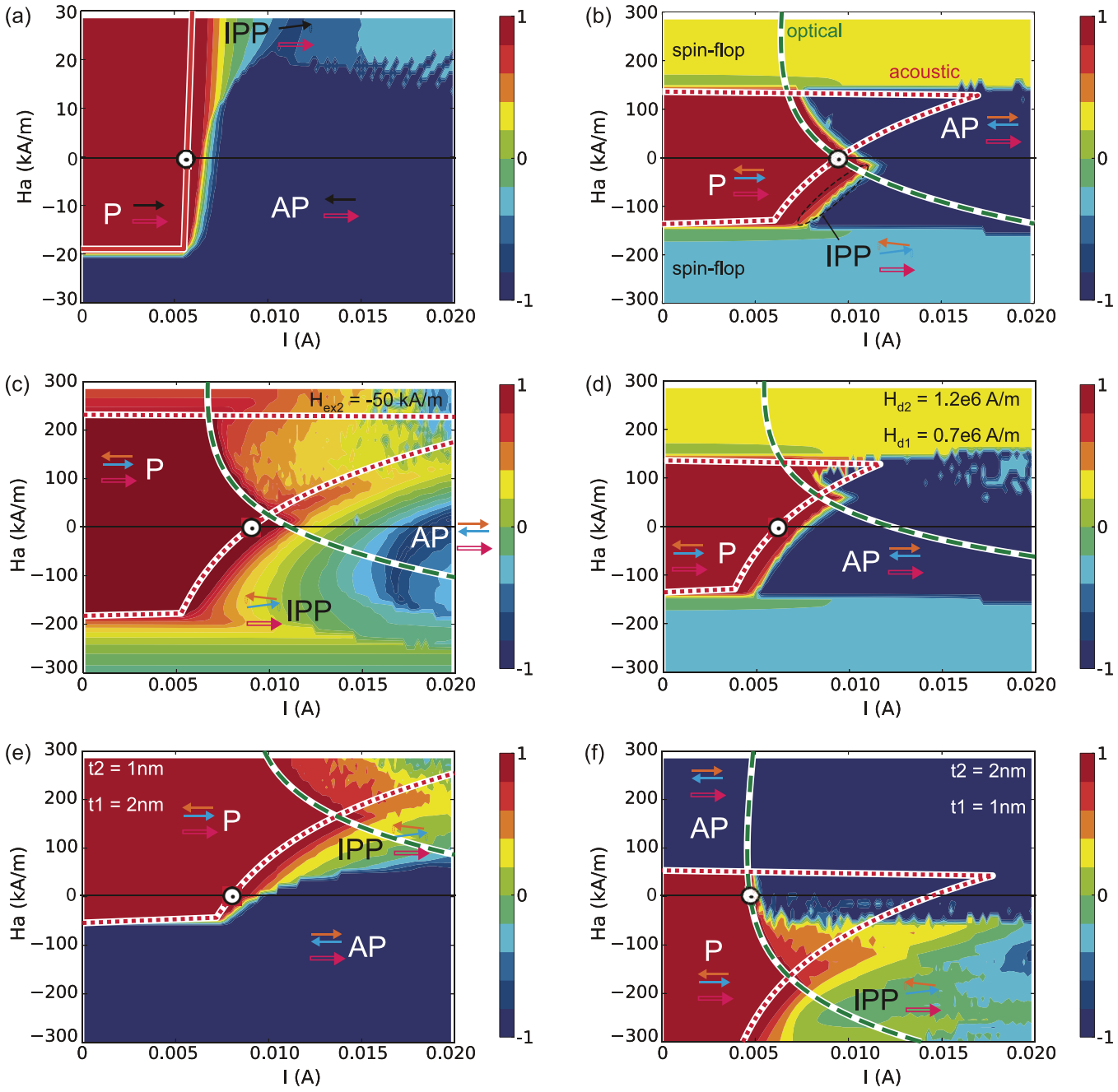

FIG. 3. (Color online) Macrospin simulations, diagram of the average $\langle m_x^1 \rangle$ between 8 and 10 ns of a 10 ns-long simulation with $m_x^1 = 1$ initially. Red dotted line, acoustic critical line. Green dashed line, optical critical line. Different configurations are represented: (a) single layer with an equivalent magnetic volume, $\alpha = 0.02$, $M_S = 1.2 \times 10^6$ A/m, $H_k = 20 \times 10^3$ A/m, $\eta_1 = 0.3$, $S = 10^{-14}$ m^2, $t = 3$ nm; and (b) identical layers, $\alpha = 0.02$, $M_S = 1.2 \times 10^6$ A/m, $H_{d1} = H_{d2} = 1.2 \times 10^6$ A/m, $H_{k1} = H_{k2} = 20 \times 10^3$ A/m, $\eta_1 = 0.3$, $S = 10^{-14}$ m^2, $t_1 = t_2 = 1.5$ nm, $J_{\mathrm{RKKY}} = -1 \times 10^{-3}$ J/m^2. Same layers with mismatch: (c) $H_{ex2} = -50$ kA/m. (d) $H_{d1} = 0.7 \times 10^6$ A/m, $H_{d2} = 1.2 \times 10^6$ A/m. (e) $t_1 = 2$ nm, $t_2 = 1$ nm. (f) $t_1 = 1$ nm, $t_2 = 2$ nm.

are the same as for the symmetric case. This exchange bias field can originate from an antiferromagnetic layer in contact with layer 2. The critical lines define the same "arrow" shape than in the symmetric case but slightly shifted towards the positive fields. The critical fields are also larger than in the symmetric case. For negative fields, the IPP range is expanded compared to the symmetric case. The critical current at zero field is slightly reduced compared to the symmetric case.

In Fig. 3(d), the demagnetizing field of layer 1 is reduced to the value $H_{d1} = 0.7 \times 10^6$ A/m. The demagnetizing field of layer 2 is unchanged. The reduced demagnetizing field can be achieved, for instance, by improving the interface between layer 1 and the MgO barrier to increase the interface perpendicular anisotropy [14]. In this case, the arrow shape of the critical lines of the two modes is shifted towards positive fields. The critical field at zero field is much reduced

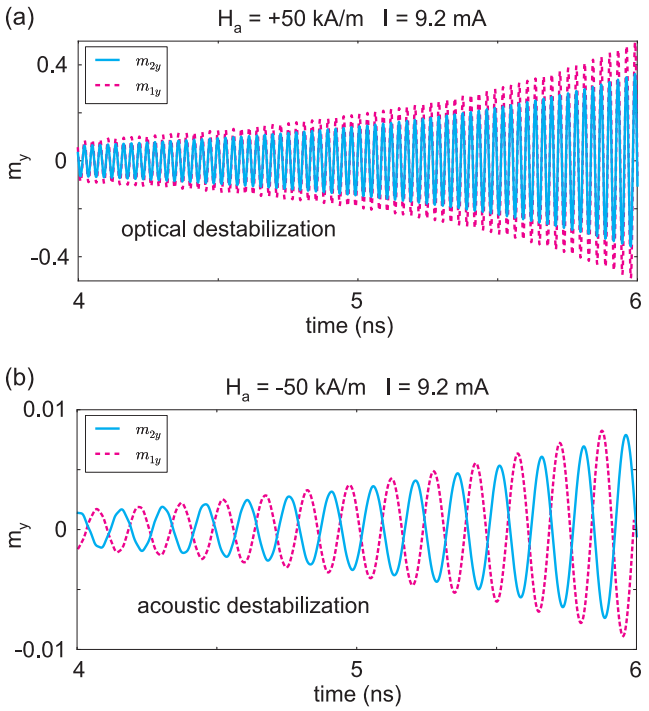

FIG. 4. (Color online) Evolution between 4 and 6 ns of the transverse in-plane components of the magnetization of the two layers, m_{1y} and m_{2y}, with an applied current density of 9.2×10^{11} A/m^2 (9.2 mA with $S = 10^{-14}$ m^2). The SyF is symmetric, corresponding to the case of Fig. 3(b). (a) Positive applied field of $H_a = 50$ kA/m: high-frequency optical destabilization. (b) Negative field of $H_a = -50$ kA/m: low-frequency acoustic destabilization.

compared to the symmetric case. Notice that the IPP region has disappeared in this case.

In Figs. 3(e) and 3(f), the two layers of the SyF have different thicknesses: $t_1 = 2$ nm, $t_2 = 1$ nm, and $t_1 = 1$ nm, $t_2 = 2$ nm, respectively. The total thickness remains 3 nm, like for the symmetric SyF and the single layer. Thus the comparison is made with systems with the same magnetic volume. The thickness asymmetry provokes a shift of the arrow shape of the critical lines, towards either positive or negative field (respectively). In both cases, the critical current at zero field is reduced compared to the symmetric case.

The present analysis does not permit to conclude on the existence or not of an IPP region. For this, a different approach should be used, based on the work of Slavin *et al.* [15]. In this theory (for single layers), not only the linear part of the LLGS equation is computed, but also the non-linear part that describes the self-sustained oscillations.

Even if the range of existence of in-plane precession (IPP) cannot be known from this equilibrium analysis, macrospin simulations show that self-sustained IPP are acoustiClike. Therefore the IPP were never encountered above the optical critical current. This is specially interesting to use SyF free layer for memory application. If we assume that the spin torque originating from the reference layer is totally transmitted to the first layer of the SyF, then in the case of an asymmetric SyF with $t_1 < t_2$ [see Fig. 3(f)], the critical current at zero field is always optical. With the other current polarity, the destabilization of the AP equilibrium is also optical. Therefore, no self-sustained oscillations (with reasonable applied currents) can be obtained at zero field. For memory application, it ensures that the magnetization of layer 1 (and layer 2 simultaneously) is reversed with an applied current larger than the critical current.

B. Decrease of the critical current of a SyF free layer

It was shown that the critical current of a SyF free layer could be reduced by introducing asymmetry in the structure. However, no quantitative comparison was given with the critical current of a single layer (SL) free layer. To investigate this, the expression of the critical currents of SyF and SL free layer will be compared in the given framework (as in Fig. 3): (i) the layers of the SyF and of the SL of comparison have the same saturation magnetization M_S (meaning that all the layers are made of the same material) and the total thickness of the SyF, $t_1 + t_2$, is equal to the thickness t of the single layer; (ii) all the layers have the same damping α and there is no spin-efficiency asymmetry ($\lambda_1 = \lambda_2 = 0$); and (iii) the spin torque originating from the reference layer is neglected on the second layer in the SyF ($i_2 = 0$). There are some evidence that the spin torque may be transferred to the second layer [12,13], however, the STT on the second layer is smaller than on the first one. Therefore it is neglected here.

A general expression for reduced demagnetizing fields is also used. The effective demagnetizing fields are reduced due to perpendicular interface anisotropies [14,16]. The interface anisotropy originates from the interface with the MgO separating the first layer from the reference layer, but also from another interface on top of the structure:

$$H_d^{\mathrm{SL}} = M_S - \frac{K_1 + K_2}{\mu_0 M_S t},$$
$$H_{d2} = M_S - \frac{K_2}{\mu_0 M_S t_2},$$
$$H_{d1} = M_S - \frac{K_1}{\mu_0 M_S t_1}.$$

With K_1 the surface anisotropy energy density due to the interface with the MgO and K_2 the one due to the top interface. We introduce the characteristic currents I_0^{SyF} and I_0^{SL}:

$$I_0^{\mathrm{SyF}} = \frac{2eS}{\hbar\eta_1}\alpha\frac{H_{d1} + H_{d2}}{2}M_S\,(2t_1),$$
$$I_0^{\mathrm{SL}} = \frac{2eS}{\hbar\eta_1}\alpha H_d^{\mathrm{SL}} M_S t.$$

We use the notation $Q = Q' + j$, so that for a single layer (SL):

$$I_c^{\mathrm{SL}} = I_0^{\mathrm{SL}}(1/2 + Q').$$

For the critical current of the SyF, we neglect the asymmetry term in the numerator of Eq. (10), so that

$$I_c^{\mathrm{SyF}} = I_0^{\mathrm{SyF}}\frac{1/2 + Q' + j}{1 + |\delta|}.$$

We use the adimensional thickness asymmetry τ:

$$t = t_2 + t_1, \quad \tau = \frac{t_2 - t_1}{t_2 + t_1}.$$

Notice that because $M_1 = M_2 = M_S$, $\tau = -\nu$.

According to the expressions of the demagnetizing fields, the ratio σ of the SyF and of the SL characteristic currents, $\sigma = I_0^{\mathrm{SyF}}/I_0^{\mathrm{SL}}$, is given by

$$\sigma = 1 - \tau\frac{1+\epsilon}{1+\tau\epsilon}.$$

Therefore the critical current for a SyF MTJ is smaller than for a single layer MTJ if the following condition is fulfilled:

$$\sigma\left(\tfrac{1}{2} + Q' + j\right) < \left(\tfrac{1}{2} + Q'\right)(1+\delta).$$

This can be written as a maximum for the adimensional RKKY coupling energy J defined earlier:

$$2J < \frac{(1+2Q')(1+\epsilon\tau)}{1-\tau} \times \left[\tau\frac{J}{j}\frac{1+\epsilon}{1+\epsilon\tau} + \left|\epsilon + \kappa(1+2Q'+2j)\right|\frac{1+Q'/j}{\sqrt{\gamma_n}}\right].$$

Two particular cases are of interest: (1) $\epsilon = 0 \Longrightarrow 2J < \frac{\tau}{1-\tau}C$ with $C = 2$ or $C = -Q'/j$ if τ is positive or negative, respectively, and (2) $\tau = 0 \Longrightarrow 2J < |\epsilon|(1+2Q')(1+Q'/j)$.

In this framework, where no spin torque is acting on layer 2 of the SyF, it appears that the critical current of a single layer can be reduced by making it a SyF with the same magnetic volume. The corresponding SyF must be strongly asymmetric, either due to the thickness difference between its two layers (Fig. 5), or due to an interfacial surface anisotropy (Fig. 6). For an asymmetric SyF, reducing the RKKY coupling energy reduces the critical current (Fig. 7).

However, these parameters also affect other properties of the SyF, like for instance the coercive field. As seen in Fig. 3(f), the coercive field for a SyF with asymmetric thicknesses, $t_1 =$ 1 nm and $t_2 = 2$ nm, is much reduced compared to a symmetric SyF: 50 kA/m compared to 150 kA/m in the symmetric case. Therefore the thickness asymmetry must not be too large, so that the MTJ has a large enough bistable region with respect to external field to avoid external perturbating fields to change its magnetization orientation.

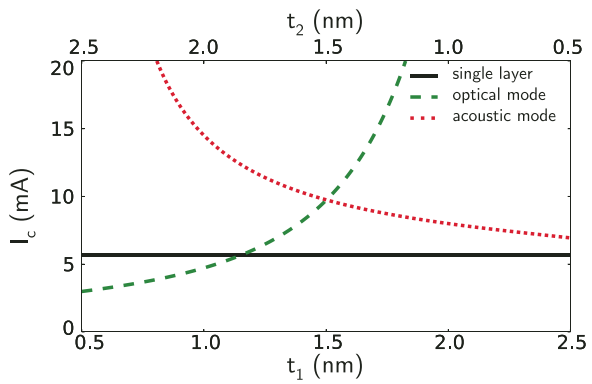

FIG. 5. (Color online) Critical current vs thickness of layer 1, t_1, for the same total thickness tt of 3 nm.

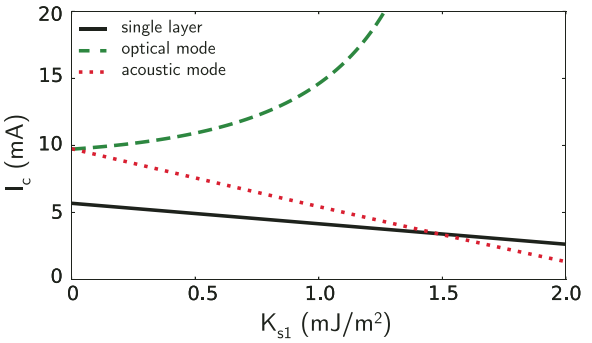

FIG. 6. (Color online) Critical current vs interfacial surface anisotropy energy of the layer 1, K_{s1}.

IV. STABILITY ANALYSIS OF SYF OSCILLATOR WITHOUT PINNED POLARIZING LAYER

Unlike the previous section, the system of interest consists in a SyF bilayer without fixed polarizing layer ($\eta_1 = \eta_2 = 0$, so $i = 0$), with antiferromagnetic coupling between the layers ($n = -1$), and with mutual spin torque between the layers, as shown in Fig. 8. The layers magnetizations are excited only by the mutual spin torque between the layers. It also provides an extra coupling between the layers, in addition to the RKKY coupling. Some experimental results on this configuration were presented in Ref. [17]. An experimental phase diagram is presented, for positive applied field, which shows that the self-sustained oscillations appear only for positive current. This feature can possibly be explained by the following analytical calculations of the critical current, because the two modes, acoustic or optical, are excited each for one polarity of the current. If only one of these modes is detected experimentally, it would explain why the excitations are only encountered for one current polarity. Moreover, the simulations show that it is possible to excite an optical-like mode in this structure. Since the optical mode has a larger frequency than the acoustic mode usually encountered in conventional STO, such structure could extend the frequency range of STO.

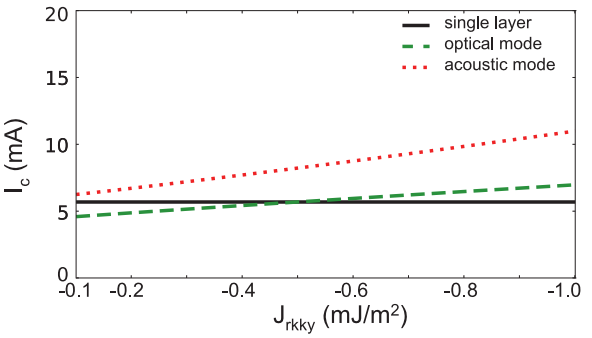

FIG. 7. (Color online) Critical current vs RKKY coupling energy J_{RKKY} with a thickness asymmetry: $t_1 = 1.3$ nm, $t_2 = 1.7$ nm.

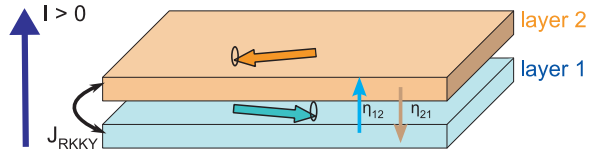

FIG. 8. (Color online) Schematics of a SyF oscillator without reference layer and with mutual spin torque between the layers.

In order to simplify the problem and try to focus on what makes this system special, the layers are supposed to be identical, hence $\epsilon = \nu = \zeta = \rho = 0$, and also $t_1 = t_2$, $j = J$. In addition, without applied field, $\kappa = 0$, and so the linewidths for the two modes, optical and acoustic, write

$$\Delta\omega_{\mathrm{op/ac}} = -\alpha\omega\left[1 + 2Q \mp \frac{2\beta\alpha^2 k^2}{j}(1 + 2Q - 2j)\right]. \quad (10)$$

The equilibrium state becomes unstable when the linewidth becomes positive, and according to the previous equation, without applied field, this is possible only for the optical mode. Notice also that without the spin-torque fieldlike term ($\beta = 0$), the linewidth is not modified by the current in the symmetric case. Because k is proportional to the applied current I, increasing the current increases the acoustic mode linewidth in absolute value but it always remains negative. However, when increasing the current, the optical mode linewidth will eventually vanish.

The critical lines corresponding to $\Delta\omega_{\mathrm{op/ac}} = 0$ are represented on the phase diagram of Fig. 9 versus applied current and applied field. Without applied field, only the optical mode can be excited. The final state of macrospin simulations are superposed to the critical lines and show a good

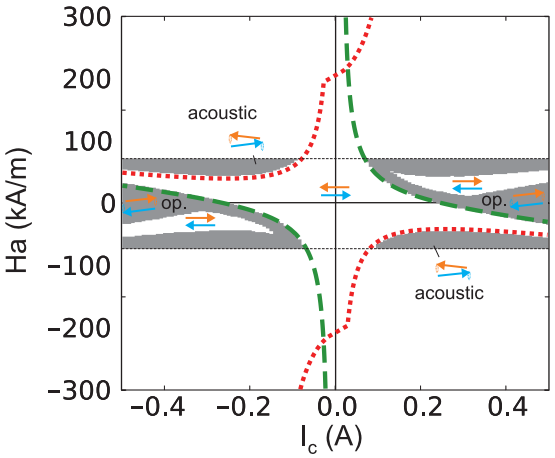

FIG. 9. (Color online) Critical lines vs current and field without fixed polarizing layer and with mutual spin torque between the layers. Red dotted line is the acoustic mode and green dashed line is the optical mode. From $H_a = -50$ to 50 kA/m, a steady state from macrospin simulations: in-plane steady state (white region) and IPP (grey region). The bottom layer of the SyF is initially along $+\boldsymbol{u}_x$ (center), and reverses to $-\boldsymbol{u}_x$ in the top right and bottom left. The IPP is optical-like around zero field and close to the optical critical line, and acousticlike otherwise. The layers are identical, with thicknesses $t_1 = t_2 = 1.5$ nm, $J_{\mathrm{RKKY}} = -10^{-3}$ J/m^2, and $\beta_{\mathrm{IEC}} = 1$.

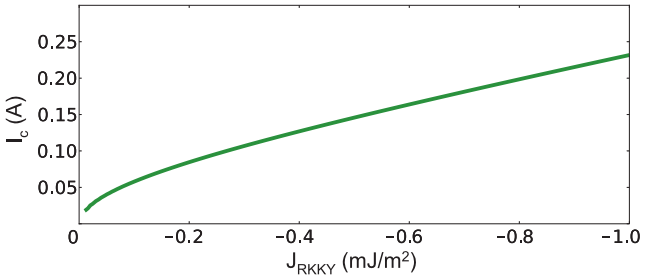

FIG. 10. (Color online) Critical current vs RKKY coupling energy J_{RKKY} without fixed polarizing layer and with mutual spin torque between the layers. The layers are identical, with $S = 10^{-14}$ m^2 and thicknesses $t_1 = t_2 = 1.5$ nm and no applied field, $H_a = 0$.

agreement. The simulation were realized on a symmetric SyF with $t_1 = t_2 = 1.5$ nm, $\alpha = 0.02$, $H_k = 20$ kA/m, $J_{\mathrm{RKKY}} = -10^{-3}$ J/m^2, $\beta_{\mathrm{IEC}} = 1$. The mutual spin polarization are equal: $\eta_{21} = \eta_{12} = 0.3$. Moreover, $\lambda_{21} = \lambda_{12} = 0$. The simulations were only performed between -50 and 50 kA/m. The bottom layer of the SyF, layer 1, is initially oriented along $+\boldsymbol{u}_x$. The two layers are antiparallel due to the RKKY coupling, $\boldsymbol{m}_1 = \boldsymbol{u}_x$ and $\boldsymbol{m}_2 = -\boldsymbol{u}_x$. The gray regions represent a final IPP steady state, with acoustic-like or optical-like oscillations, depending on the region. The borders acoustic/optical inside the gray region were not calculated, only the mode just above the critical current was identified. The white regions represent an equilibrium state, either $\boldsymbol{m}_1 = +\boldsymbol{u}_x$ below the critical current, or $\boldsymbol{m}_1 = -\boldsymbol{u}_x$ for two regions above the critical current. The latter $\boldsymbol{m}_1 = -\boldsymbol{u}_x$ reversed regions cannot be predicted by the linear analysis presented in this paper.

The expressions of the critical lines are complicated with an applied field, however, it is possible to obtain the expression of the critical current for $H_a = 0$ (and $H_{ex1} = H_{ex2} = 0$).

Let I_m be a characteristic current amplitude, given by

$$I_m = \alpha M_s t_1 \frac{2e\omega S}{\gamma\hbar}\frac{1 - \lambda_{21}}{\eta_{21}}, \quad (11)$$

The critical current I_c^{op} of two identical layers with mutual spin torque and without applied field is given by

$$I_c^{\mathrm{op}} = \frac{I_m}{\alpha}\sqrt{\frac{j}{2\beta_{\mathrm{IEC}}}}\sqrt{\frac{1 + 2Q}{1 + 2Q - 2j}}. \quad (12)$$

Because j is proportional to the RKKY coupling energy per unit area J_{RKKY}, it appears that the critical current is proportional to the square root of the RKKY coupling constant for small coupling, as shown in Fig. 10. Notice that the RKKY constant is also included in Q, therefore for a large RKKY constant, namely, $j > 1/2$, the critical current tends to be proportional to j.

V. CONCLUSION

The analysis of the equilibrium stability of an in-plane SyF free layer with reference layer was performed. The expressions of the FMR frequency and linewidth were extracted. They were found to be different for the two modes, optical and acoustic. Consequently, the critical currents in a SyF, defined

by the vanishing of the FMR linewidth, can be of two different types, acoustic or optical, depending on which linewidth vanishes. The type of critical current can be selected by tuning, for example, the thicknesses of the two layers composing a SyF.

In a symmetric SyF, the critical current (either acoustic or optical) is generally larger than the critical current of a single layer free layer with equivalent magnetic volume. This is due to the RKKY coupling energy. However, we showed that the critical current of a strongly asymmetric SyF could be reduced below the value of the equivalent single layer. This opens new perspectives to reduce the critical current in magnetic random-access memories.

Finally, we studied the system composed of an in-plane SyF with mutual spin torque between the two layers and without reference layer. In this configuration, and for a symmetric SyF, we found that only the optical mode can be excited at zero field. It is qualitatively different from conventional STO, for which the self-sustained oscillations are acousticlike. Moreover, the IEC, or fieldlike spin torque, was found to play a preponderant role in the excitation of such mutual spin-torque oscillators.

ACKNOWLEDGMENT

This work was supported by the European commission through the ERC Adv Grant HYMAGINE No. 246942.

APPENDIX A: EQUATION OF MOTION AND SPIN TRANSFER TORQUES

The spin transfer torque was introduced by Slonczewski [1] and Berger [2], as an additional torque in the Landau-Lifshitz-Gilbert (LLG) equation that describe the dynamics of the magnetization $\boldsymbol{m}$ of a single layer:

$$\begin{aligned}\dot{\boldsymbol{m}} &= -\mu_0\gamma\,\boldsymbol{m}\times\boldsymbol{H}_{\text{eff}} + \alpha\boldsymbol{m}\times\dot{\boldsymbol{m}} + \mu_0\gamma\boldsymbol{\tau}_{\text{STT}},\\ \boldsymbol{H}_{\text{eff}} &= \frac{-1}{\mu_0 M_S V}\frac{\partial E}{\partial \boldsymbol{m}},\\ \boldsymbol{\tau}_{\text{STT}} &= a_J\,\boldsymbol{m}\times(\boldsymbol{m}\times\boldsymbol{M}_{\text{pol}}) + b_J\boldsymbol{m}\times\boldsymbol{M}_{\text{pol}},\end{aligned}$$

where E is the free energy of the layer, M_S is the saturation magnetization, V is the volume of the layer, α is the damping constant, and γ is the gyromagnetic ratio.

Regarding the spin-torque terms, $\boldsymbol{M}_{\text{pol}}$ is the unit vector of the magnetization direction of the fixed polarizing layer, situated after the free layer according to the current direction. b_J represents the interlayer exchange coupling (IEC), or fieldlike term. a_J is the spin torque amplitude given by the general expression

$$a_j = \frac{\hbar}{2e}\frac{I}{\mu_0 M_S V}\,\frac{\eta}{1+\lambda\boldsymbol{m}\cdot\boldsymbol{M}_{\text{pol}}}.$$

Here, I is the applied current, η is the spin polarization of the current due to the polarizing layer, and λ is the spin-efficiency asymmetry, that depends on the spacer between the free layer and the polarizing layer. It can be considered to be zero for a tunnel barrier and nonvanishing for metallic spacers.

Like for the effective field $\boldsymbol{H}_{\text{eff}}$, which derives from the free energy, it is interesting to write the STT as the gradient of a potential. In this way, the change of basis are much simplified. The torque itself cannot derive from a potential, however, we can define the potential P, such that

$$\begin{aligned}a_J\boldsymbol{M}_{\text{pol}} &= \frac{-1}{\mu_0 M_S V}\frac{\partial P}{\partial \boldsymbol{m}},\\ P &= -\frac{\hbar}{2e}\frac{I\eta}{\lambda}\ln(1+\lambda\boldsymbol{m}\cdot\boldsymbol{M}_{\text{pol}}).\end{aligned}$$

Therefore we transform the LLG equation to eliminate the $\dot{\boldsymbol{m}}$ term from the right-hand side and we assumed that $\gamma/(1+\alpha^2)\approx\gamma$:

$$\begin{aligned}\dot{\boldsymbol{m}} = \frac{\gamma}{M_S V}\boldsymbol{m}\times\left(\partial_{\boldsymbol{m}}E + \alpha\partial_{\boldsymbol{m}}P - \frac{b_J}{a_J}\partial_{\boldsymbol{m}}P\right) + \frac{\gamma}{M_S V}\boldsymbol{m}\\ \times\left[\boldsymbol{m}\times\left(\alpha\partial_{\boldsymbol{m}}E - \partial_{\boldsymbol{m}}P - \alpha\frac{b_J}{a_J}\partial_{\boldsymbol{m}}P\right)\right].\end{aligned}$$

The first term is the conservative part of the LLG equation. For compactness, we introduce a coefficient β that accounts for the STT term of the conservative part:

$$\alpha\beta = \alpha - \frac{b_J}{a_J}. \tag{A1}$$

With this notation, β vanishes if the STT is neglected in the conservative part. It is unity if the intrinsic IEC, b_J, is neglected, for example, in spin valves. b_J has a quadratic dependence to the applied current, whereas a_J is linear with respect to the current [18]. Therefore β may depend on the applied current.

The second term in Eq. (A1) is the dissipative term. We neglect the contribution from b_J, as we suppose that $\alpha\frac{b_J}{a_J}\ll 1$. This assumption is justified by the maximal value encountered in MTJ for b_J, which is 30% the value of a_J. The damping constant is supposed to be small, $\alpha < 0.1$.

The LLG equation rewrites as

$$\begin{aligned}\dot{\boldsymbol{m}} = \frac{\gamma}{M_S V}\boldsymbol{m}\times\partial_{\boldsymbol{m}}(E+\alpha\beta P) + \frac{\gamma}{M_S V}\boldsymbol{m}\\ \times[\boldsymbol{m}\times\partial_{\boldsymbol{m}}(\alpha E - P)].\end{aligned} \tag{A2}$$

APPENDIX B: DYNAMICAL MATRIX

The Landau-Lifshitz-Gilbert-Slonczewski (LLGS) vectorial equation for a SyF free layer has four degrees of freedom, therefore it may be more convenient to write it in spherical coordinates instead of cartesian coordinates. We use the angles θ_1, ϕ_1, θ_2, and ϕ_1:

$$\begin{aligned}m_x^1 &= \sin\theta_1\cos\phi_1, & m_x^2 &= \sin\theta_2\cos\phi_2,\\ m_y^1 &= \sin\theta_1\sin\phi_1, & m_y^2 &= \sin\theta_2\sin\phi_2,\\ m_z^1 &= \cos\theta_1, & m_z^2 &= \cos\theta_2.\end{aligned}$$

We also introduce the following scalar functions related to the one introduced in Appendix A:

$$\mathcal{H}_1 = \frac{\gamma}{M_1 V_1}(E + \beta\alpha_1 P_1), \quad \Gamma_1 = \frac{\gamma}{M_1 V_1}(\alpha_1 E - P_1),$$

$$\mathcal{H}_2 = \frac{\gamma}{M_2 V_2}(E + \beta\alpha_2 P_2), \quad \Gamma_2 = \frac{\gamma}{M_2 V_2}(\alpha_2 E - P_2).$$

In the spherical coordinates, using the previous scalar functions, the LLGS equation rewrites

$$\begin{pmatrix} \dot{\theta}_1 \\ \sin\theta_1 \dot{\phi}_1 \end{pmatrix} = \mathbf{\Omega_1}\, \partial_{\vec{R}_1} \mathcal{H}_1 - \partial_{\vec{R}_1} \Gamma_1,$$

$$\begin{pmatrix} \dot{\theta}_2 \\ \sin\theta_2 \dot{\phi}_2 \end{pmatrix} = \mathbf{\Omega_1}\, \partial_{\vec{R}_2} \mathcal{H}_2 - \partial_{\vec{R}_2} \Gamma_2,$$

$$\mathbf{\Omega_1} = \begin{pmatrix} 0 & -1 \\ 1 & 0 \end{pmatrix}, \quad \partial_{\vec{R}_i} = \begin{pmatrix} \frac{\partial}{\partial\theta_i} \\ \frac{1}{\sin\theta_i}\frac{\partial}{\partial\phi_i} \end{pmatrix} \text{ for } i \in (1,2).$$

To study the stability of equilibriums, we need to differentiate the right-hand side of the LLGS equation, to obtain the 4×4 dynamical matrix that we call L. The expression of L in spherical coordinates is given by

$$L = \begin{pmatrix} \mathbf{\Omega_1} & \mathbf{0} \\ \mathbf{0} & \mathbf{\Omega_1} \end{pmatrix} \mathbf{Hess}[\mathcal{H}_1, \mathcal{H}_2] - \mathbf{Hess}[\Gamma_1, \Gamma_2].$$

Inside the block matrix, $\mathbf{0}$ is the 2×2 null matrix.

For two arbitrary scalar functions A and B, the 4×4 matrix called $\mathbf{Hess}[A, B]$ is defined further, when the equilibrium configuration is assumed to be in-plane ($\cos\theta_1 = \cos\theta_2 = 0$). The standard notation for the second derivative, $A_{\theta_1\phi_2} = \frac{\partial^2 A}{\partial\theta_1 \partial\phi_2}$, is used. The second derivatives are then evaluated in the equilibrium configuration, $\cos\theta_1 = \cos\theta_2 = 0$, $\cos\phi_1 = m$, and $\cos\phi_2 = nm$:

$$\mathbf{Hess}[A, B] = \begin{pmatrix} A_{\theta_1\theta_1} & A_{\theta_1\phi_1} & A_{\theta_1\theta_2} & A_{\theta_1\phi_2} \\ A_{\theta_1\phi_1} & A_{\phi_1\phi_1} & A_{\phi_1\theta_2} & A_{\phi_1\phi_2} \\ B_{\theta_1\theta_2} & B_{\phi_1\theta_2} & B_{\theta_2\theta_2} & B_{\theta_2\phi_2} \\ B_{\theta_1\phi_2} & B_{\phi_1\phi_2} & B_{\theta_2\phi_2} & B_{\phi_2\phi_2} \end{pmatrix}.$$

APPENDIX C: ANNEXE

Several parameters are common to all the graphs presented in this paper. For instance, the saturation magnetizations M_s and the anisotropy fields H_k. The following table presents the parameters used for Figs. 3(a) and 3(b).

Single layer	SyF	Value
M_s	M_{s1}, M_{s2}	1.2×10^6 A/m
H_k	H_{k1}, H_{k2}	20×10^3 A/m
α	α_1, α_2	0.02
t	t_1, t_2	3 nm (1.5-1.5 nm SyF)
S		100×100 nm^2 $= 10^{-14}$ m^2
η	η_1	0.3
	η_2	0
–	$\eta_{21} = \eta_{12}$	0.3
λ	$\lambda_1, \lambda_2, \lambda_{12}, \lambda_{21}$	0
β		1

According to the value of the area S of the pillars, currents expressed in mA correspond to current densities of 10^{11} A/m^2.

[1] J. C. Slonczewski, J. Magn. Magn. Mater. **159**, L1 (1996).
[2] L. Berger, Phys. Rev. B **54**, 9353 (1996).
[3] J. A. Katine, F. J. Albert, R. A. Buhrman, E. B. Myers, and D. C. Ralph, Phys. Rev. Lett. **84**, 3149 (2000).
[4] J. Z. Sun, Phys. Rev. B **62**, 570 (2000).
[5] M. Tsoi, A. G. M. Jansen, J. Bass, W. C. Chiang, M. Seck, V. Tsoi, and P. Wyder, Phys. Rev. Lett. **80**, 4281 (1998).
[6] S. Cornelissen, L. Bianchini, T. Devolder, J.-V. Kim, W. Van Roy, L. Lagae, and C. Chappert, Phys. Rev. B **81**, 144408 (2010).
[7] D. Gusakova, D. Houssameddine, U. Ebels, B. Dieny, L. Buda-Prejbeanu, M. C. Cyrille, and B. Delaet, Phys. Rev. B **79**, 104406 (2009).
[8] E. Monteblanco, D. Gusakova, J. F. Sierra, L. D. Buda-Prejbeanu, and U. Ebels, IEEE Magn. Lett. **4**, 3500204 (2013).
[9] T. Devolder and K. Ito, J. Appl. Phys. **111**, 123914 (2012).
[10] P. Baláž and J. Barnaś, Phys. Rev. B **88**, 014406 (2013).
[11] B. Lacoste, L. D. Buda-Prejbeanu, U. Ebels, and B. Dieny, Phys. Rev. B **88**, 054425 (2013).
[12] M. Ichimura, T. Hamada, H. Imamura, S. Takahashi, and S. Maekawa, J. Appl. Phys. **105**, 07D120 (2009).
[13] M. Ichimura, T. Hamada, H. Imamura, S. Takahashi, and S. Maekawa, J. Appl. Phys. **109**, 07C906 (2011).
[14] S. Monso, B. Rodmacq, S. Auffret, G. Casali, F. Fettar, B. Gilles, B. Dieny, and P. Boyer, Appl. Phys. Lett. **80**, 4157 (2002).
[15] A. Slavin and V. Tiberkevich, IEEE Trans. Magn. **44**, 1916 (2008).
[16] P. Khalili Amiri, Z. M. Zeng, J. Langer, H. Zhao, G. Rowlands, Y.-J. Chen, I. N. Krivorotov, J.-P. Wang, H. W. Jiang, J. A. Katine, Y. Huai, K. Galatsis, and K. L. Wang, Appl. Phys. Lett. **98**, 112507 (2011).
[17] T. Seki, H. Tomita, M. Shiraishi, T. Shinjo, and Y. Suzuki, Appl. Phys. Exp. **3**, 033001 (2010).
[18] I. Theodonis, N. Kioussis, A. Kalitsov, M. Chshiev, and W. H. Butler, Phys. Rev. Lett. **97**, 237205 (2006).